2007 IEEE International Conference on
Robotics and Automation
Roma, Italy, 10-14 April 2007

An accurate closed-form estimate of ICP's covariance

Andrea Censi

Università degli Studi di Roma "La Sapienza"
Dipartimento di Informatica e Sistemistica "A. Ruberti"
via Eudossiana 18, I-00184 Rome, Italy
andrea.censi@dis.uniroma1.it

***Abstract*— Existing methods for estimating the covariance of the ICP (Iterative Closest/Corresponding Point) algorithm are either inaccurate or are computationally too expensive to be used online. This paper proposes a new method, based on the analysis of the error function being minimized. It considers that the correspondences are not independent (the same measurement being used in more than one correspondence), and explicitly utilizes the covariance matrix of the measurements, which are not assumed to be independent either. The validity of the approach is verified through extensive simulations: it is more accurate than previous methods and its computational load is negligible. The ill-posedness of the surface matching problem is explicitly tackled for under-constrained situations by performing an observability analysis; in the analyzed cases the method still provides a good estimate of the error projected on the observable manifold.**

I. Introduction

The ICP (Iterative Closest/Corresponding Point) algorithm is used in a variety of problems. This paper addresses in particular the *localization* and *scan matching* problems that arise in mobile robotics, for which a precise covariance estimate is needed.

The inputs for the localization problem are: a known map S_{ref}, a sensor scan $\boldsymbol{y}_t$, and the odometry estimate $\boldsymbol{u}$. The inputs for scan matching are: a reference scan $\boldsymbol{y}_{t-1}$, a sensor scan $\boldsymbol{y}_t$, and $\boldsymbol{u}$. The input data $\boldsymbol{y}$ and $\boldsymbol{u}$ are modelled as random variables with known statistical properties. Let $\boldsymbol{x} = (x, y, \theta)$ be the roto-translation between the two poses of the robot (Fig. 1). Then a scan matching algorithm is a function A of the input data that returns an estimate of $\boldsymbol{x}$: $\hat{\boldsymbol{x}} = A(\boldsymbol{y}_{t-1}, \boldsymbol{y}_t, \boldsymbol{u})$. The output $\hat{\boldsymbol{x}}$ is itself a random variable. To correctly integrate the scan matching estimate in a SLAM algorithm, it is needed to know its statistical properties: the bias $E\{A\} - \boldsymbol{x}$, and the covariance $\operatorname{cov}(\hat{\boldsymbol{x}}) \triangleq$

$$E\Big\{\big[A(\boldsymbol{y}_{t-1}, \boldsymbol{y}_t, \boldsymbol{u}) - E\{A\}\big]\big[A(\boldsymbol{y}_{t-1}, \boldsymbol{y}_t, \boldsymbol{u}) - E\{A\}\big]^{\mathsf{T}}\Big\} \quad (1)$$

In SLAM, the covariance is needed to fuse the estimate with other sensors, to obtain a proposal distribution for particle filters, and to weight constraints in a pose-graph.

The most rigorous study of the covariance estimation problem has been developed in [1], [2]: nevertheless, the two methods proposed there (the *Hessian method* and the *Offline method*) have some drawbacks. The closed-form Hessian method over-estimates the covariance in some cases. The Offline method gives reasonable results but cannot be used online, as it is based on a computationally expensive procedure. The method presented here has a closed form and is more accurate.

A. ICP for localization and scan matching

Algorithms of the ICP family solve localization and scan-matching by formulating a *surface matching* problem, whose inputs are a surface S_{ref}, a set of points $\{\boldsymbol{p}_k\}$, and a starting guess. This formulation can accommodate both localization and scan matching. In the first case, S_{ref} is given, while in the second S_{ref} can be approximated by a polyline connecting the points in $\boldsymbol{y}_{t-1}$ (Fig. 1).

The basic surface matching problem is to find an $\boldsymbol{x}$ that minimizes the following error function:

$$J(S_{\text{ref}}, \{\boldsymbol{p}_k\}, \boldsymbol{x}) = \sum_k \left\| \mathbf{T}_{\boldsymbol{x}} \boldsymbol{p}_k - \Pi(S_{\text{ref}}, \mathbf{T}_{\boldsymbol{x}} \boldsymbol{p}_k) \right\|^2 \quad (2)$$

Here $\mathbf{T}_{\boldsymbol{x}} \boldsymbol{p}_k$ indicates the point $\boldsymbol{p}_k$ roto-translated by $\boldsymbol{x}$, and $\Pi(S_{\text{ref}}, \mathbf{T}_{\boldsymbol{x}} \boldsymbol{p}_k)$ is the projection of $\mathbf{T}_{\boldsymbol{x}} \boldsymbol{p}_k$ onto the surface S_{ref}. ICP minimizes (2) iteratively: at each step it computes a set of correspondences $\{(\boldsymbol{p}_k, \boldsymbol{q}_k)\}$ with $\boldsymbol{p}_k$ being one of the sensor points and $\boldsymbol{q}_k = \Pi(S_{\text{ref}}, \mathbf{T}_{\boldsymbol{x}_{\text{OLD}}} \boldsymbol{p}_k)$ lying on the surface S_{ref}; then an incremental solution is found for $\boldsymbol{x}_{\text{NEW}}$ that minimizes $\sum_k \left\| \mathbf{T}_{\boldsymbol{x}_{\text{NEW}}} \boldsymbol{p}_k - \boldsymbol{q}_k \right\|^2$. This process is repeated until convergence.

Since its introduction in the early '90s, the ICP has evolved in numerous variants [3], with also several specializations for robotics SLAM (e.g. [4], [5], [6]). This paper considers the 'vanilla' ICP with the error metric defined as in (2); however, the results should be valid for other variants as well. In fact, the proposed method does not make any specific assumption on the algorithm itself, and it is based only on the analysis of the error metric being minimized.

B. Sources of error for ICP

There are three main sources of error for ICP.

The first source of error is **wrong convergence**: ICP can converge to a local minimum out of the attraction area of the 'true' solution. It is essentially unavoidable. In fact, an iterative method cannot be *complete,* as there are situations in which two equally likely solutions exists. This kind of error is very hard to model, because global convergence results do not exist for ICP.

In this paper it is assumed that the algorithm is not trapped in a local minimum, and it converges to the attraction area of the 'true' solution.

TABLE I – SYMBOLS USED IN THIS PAPER

$\boldsymbol{s}_{t-1}$	Initial pose of the robot (relative to world frame), at which the scan $\boldsymbol{y}_{t-1}$ is taken.
$\boldsymbol{x}$	Roto-translation between two consecutive poses, to be estimated with scan matching. (relative to robot frame at $t-1$).
$\boldsymbol{s}_t$	Second pose of the robot ($\boldsymbol{s}_{t-1} \oplus \boldsymbol{x} = \boldsymbol{s}_t$), at which the scan $\boldsymbol{y}_t$ is taken.
$\boldsymbol{y}_t, \boldsymbol{y}_{t-1}$	Sensor scans used to estimate $\boldsymbol{x}$.
$\boldsymbol{u}$	Odometry estimate of $\boldsymbol{x}$.
$\boldsymbol{z}$	All the measurements involved: $\boldsymbol{z} \triangleq \{\boldsymbol{y}_t, \boldsymbol{y}_{t-1}\}$.
$\check{\boldsymbol{z}}$	Actual measurements observed.
$\hat{\boldsymbol{x}} = A(\check{\boldsymbol{z}})$	Estimate of $\boldsymbol{x}$ obtained using algorithm A.
$J(\boldsymbol{z}, \boldsymbol{x})$	Error function minimized by algorithm A.
$\boldsymbol{\mathcal{I}}(\boldsymbol{x})$	Fisher's information matrix.
$\Pi(S, \boldsymbol{p})$	Euclidean projection of $\boldsymbol{p}$ onto set S
$\mathbf{T}_{\boldsymbol{x}}\boldsymbol{p}$	Point $\boldsymbol{p}$ transformed by a roto-translation $\boldsymbol{x}$. If $\boldsymbol{x} = (x, y, \boldsymbol{p})$, then $\mathbf{T}_{\boldsymbol{x}}\boldsymbol{p} \triangleq \boldsymbol{R}(\theta)\boldsymbol{p} + [x \;\; y]^{\mathrm{T}}$.
$\boldsymbol{v}(\phi)$	$\triangleq [\cos\phi \quad \sin\phi]^{\mathrm{T}}$
$\tilde{\rho}_i \in \mathbb{R}_+$	Measurement for the i-th ray.
φ_i	Angle of the i-th ray (relative to robot frame).
$\boldsymbol{p}$	Cartesian point corresponding to the polar measurements: $\boldsymbol{p} = \tilde{\rho}\boldsymbol{v}(\varphi)$
S_{ref}	Reference surface. In the case of scan matching, it is created by connecting the points in $\boldsymbol{y}_{t-1}$.
(i^k, j_1^k, j_2^k)	Indexes for the three points used in the k-th correspondence (i in $\boldsymbol{y}_t$, j in $\boldsymbol{y}_{t-1}$).

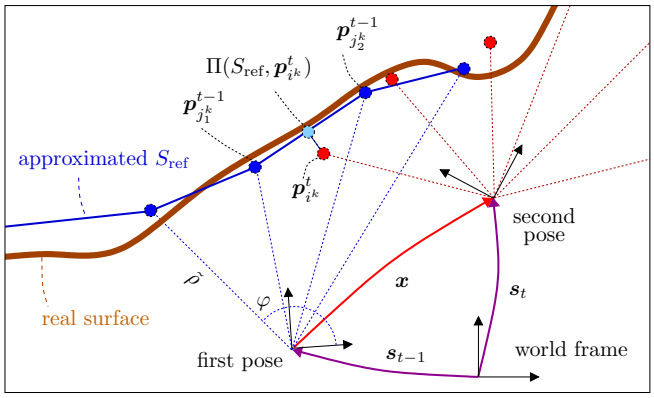

Fig. 1. Geometry of the scan matching process. Note that in ICP there are three sensor points involved in each correspondence: one from the second scan and two from the reference scan.

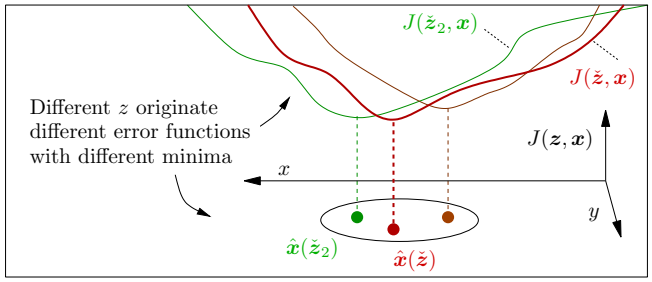

Fig. 2. Some methods for estimating the covariance [7], [1], [8] are based on the analysis of the error function for the observed measurements. Actually, one must consider *how the error function changes,* and consequently the minimum moves: this is only loosely related to the shape of the error function at a particular observed $\boldsymbol{z}$. Mathematically, the shape at a particular $\boldsymbol{z}$ is given by $\partial^2 J/\partial \boldsymbol{x}^2$; the change in the shape is contained in the quantity $\partial J/\partial \boldsymbol{z}$, which is explicitly used by the proposed method.

The second source of error are **under-constrained situations**: in some environments there is not enough information to estimate the pose of the robot completely. Apart from degenerate situations, such as having only 0, 1, or 2 distinct correspondences, in the bidimensional case the two prototypical under-constrained situations are the corridor and the circular environment (Fig. 4).

It will be shown how it is possible to check for the under-constrained situations by examining the Fisher's information matrix (derived in [9]).

The third source of error is **sensor noise**: even though ICP arrives in the attraction area of the 'true' solution, the outcome is different because of noise. It should be noted that, in constrained situations, this error is independent of the odometry error. In fact, it is found experimentally that this error exists even if the first guess coincides with the true solution. This error is theoretically justified by the existence of a lower bound for the covariance of any estimator. For the case of localization (S_{ref} is a perfect map), in [9] it is derived the Cramér–Rao lower bound (CRB). The CRB gives a good approximation to the covariance of the ICP in localization, but it is optimistic for scan matching.

The error due to sensor noise is the object of study of this paper. The approach presented here computes the covariance of this error as a function of the error metric used.

II. EXISTING APPROACHES FOR ESTIMATING ICP'S COVARIANCE

A. The "points-as-landmarks" method

This technique is used in [10], [4], [5]. The idea is to consider each correspondence as a landmark observation. [5] proposed a more complex analysis of the errors, where the covariance is based both on the sensor model and on the structure of the environment. A covariance matrix $P_{ij}^k = P_i^k + P_j^k$ is computed for each correspondence as the sum of the two point covariances, expressed in the same coordinate frame. The final covariance matrix is estimated as

$$\operatorname{cov}(\hat{\boldsymbol{x}}) \simeq \Big[\sum_k \big(P_{ij}^k\big)^{-1}\Big]^{-1} \tag{3}$$

One problem with this approach is that point correspondences are not independent observations, as more than two sensor points are used in each correspondence (Fig. 1). [1] shows that in practice this kind of estimate is very optimistic.

B. Black-box methods

The approach proposed in [1], [7], [8] is to estimate the covariance by examining the shape of the error function.

The "Hessian" method (proposed in [1]): The idea is that if the error function was a quadratic: $J(\check{\boldsymbol{z}}, \boldsymbol{x}) \simeq (Y - M\boldsymbol{x})^{\mathrm{T}}(Y - M\boldsymbol{x})$, then the optimal least-squares estimate would be $\hat{\boldsymbol{x}} = (M^{\mathrm{T}}M)^{-1}M^{\mathrm{T}}Y$ with a covariance equal to

$$\operatorname{cov}(\hat{\boldsymbol{x}}) = \left(\frac{1}{2}\frac{\partial^2}{\partial \boldsymbol{x}^2} J(\check{\boldsymbol{z}}, \boldsymbol{x})\right)^{-1} \sigma^2 \tag{4}$$

An unbiased estimate s^2 of σ^2 in (4) would be $s^2 = J(\check{\boldsymbol{z}}, \hat{\boldsymbol{x}})/(K-3)$, where K is the number of correspondences.

The final expression for the covariance estimate is

$$\mathrm{cov}(\hat{\boldsymbol{x}}) \simeq 2\frac{J(\check{\boldsymbol{z}},\hat{\boldsymbol{x}})}{K-3}\left[\frac{\partial^2}{\partial \boldsymbol{x}^2}J(\check{\boldsymbol{z}},\boldsymbol{x})\right]^{-1}_{\boldsymbol{x}=\hat{\boldsymbol{x}}} \quad (5)$$

[1] shows that this method in some cases greatly over-estimates the true covariance.

Sampling the error function: If the error function is not described analytically or it is not smooth, a robust estimate of the curvature of the error function can be obtained by sampling such function around the minimum [7], [8]. Once the estimate of the Hessian is obtained, the same reasoning can be applied to obtain the covariance estimate.

The problem with these approaches is that the shape of the error function for one particular observed $\boldsymbol{z}$ does not contain all the information needed to compute the covariance. Consider Fig. 2 which shows a bidimensional version of the problem. The estimate $\hat{\boldsymbol{x}}$ is the minimum of the error function $J(\check{\boldsymbol{z}},\boldsymbol{x})$ which depends on the observed data $\check{\boldsymbol{z}}$. If another data $\check{\boldsymbol{z}}_2$ had been observed, a different error function $J(\check{\boldsymbol{z}}_2,\boldsymbol{x})$ would have been produced, with a different minimum $\hat{\boldsymbol{x}}_2$. The covariance of $\hat{\boldsymbol{x}}$ describes the change of the position of the minimum of J if other $\boldsymbol{z}$ were observed; this is only loosely related to the shape of J at a particular $\boldsymbol{z}$. The approach proposed in this paper does consider the change in J due to noise in $\boldsymbol{z}$ (that is, $\partial J/\partial \boldsymbol{z}$).

C. The "brute force" approach

This simulation-based approach was proposed in [1]:

1) Read the first scan $\boldsymbol{y}_{t-1}$, taken at pose $\boldsymbol{s}_{t-1}$.
2) Create a map $\tilde{S}_{\text{ref}}$ from $\boldsymbol{y}_{t-1}$ by connecting consecutive points if their distance is below a threshold.
3) Repeat these steps 100 times:
   a) Choose a random displacement $\overline{\boldsymbol{x}}$ according to an error distribution.
   b) Simulate a new scan $\tilde{\boldsymbol{y}}_t$ by ray-tracing map $\tilde{S}_{\text{ref}}$ from position $\boldsymbol{s}_t = \boldsymbol{s}_{t-1} \oplus \overline{\boldsymbol{x}}$.
   c) Match $\tilde{\boldsymbol{y}}_t$ to $\boldsymbol{y}_{t-1}$ and store the matching error $(\hat{\boldsymbol{x}} - \overline{\boldsymbol{x}})$.
4) Compute the covariance matrix on the basis of the matching errors.

The main problem with this approach is that it is not possible to simulate other scans accurately because the map is not known. Moreover, it might be impossible to run the algorithm online, because of the heavy computational requirements.

III. The covariance matrix of a minimization algorithm

The following is a known method in the statistical and vision communities (see for example [11] for a similar approach).

Proposition 1: Let $\hat{\boldsymbol{x}}$ be the result of an algorithm A minimizing an error function J, which depends on the measurements $\check{\boldsymbol{z}}$: $\hat{\boldsymbol{x}} = A(\check{\boldsymbol{z}}) = \arg\min_{\boldsymbol{x}} J(\check{\boldsymbol{z}},\boldsymbol{x})$. Then the covariance of $\hat{\boldsymbol{x}}$ can be approximated as

$$\mathrm{cov}(\hat{\boldsymbol{x}}) \simeq \left(\frac{\partial^2 J}{\partial \boldsymbol{x}^2}\right)^{-1}\frac{\partial^2 J}{\partial \boldsymbol{z}\partial \boldsymbol{x}}\mathrm{cov}(\boldsymbol{z})\frac{\partial^2 J}{\partial \boldsymbol{z}\partial \boldsymbol{x}}^{\mathrm{T}}\left(\frac{\partial^2 J}{\partial \boldsymbol{x}^2}\right)^{-1} \quad (6)$$

where everything is computed at $\hat{\boldsymbol{x}}, \check{\boldsymbol{z}}$.

Proof: The first-order approximation to the covariance is

$$\mathrm{cov}(\hat{\boldsymbol{x}}) \simeq \frac{\partial A}{\partial \boldsymbol{z}}\mathrm{cov}(\boldsymbol{z})\frac{\partial A}{\partial \boldsymbol{z}}^{\mathrm{T}} \quad (7)$$

Since A is not in closed-form, it is not easy to compute $\partial A/\partial \boldsymbol{z}$. However, $A(\boldsymbol{z})$ and $\boldsymbol{z}$ are bound by an implicit function. In fact $\hat{\boldsymbol{x}}$ is a stationary point of J; a necessary condition is that the gradient is null at $\hat{\boldsymbol{x}}$: $\partial J(\check{\boldsymbol{z}},\hat{\boldsymbol{x}})/\partial \boldsymbol{x} = \boldsymbol{0}^{\mathrm{T}}$. In this case, the implicit function theorem gives an expression for $\partial A/\partial \boldsymbol{z}$. Apply the theorem (see the Appendix) with $F = \partial J/\partial \boldsymbol{x}$, $f(\boldsymbol{z}) = A(\boldsymbol{z}), \boldsymbol{x}_0 = \hat{\boldsymbol{x}}$ to obtain

$$\left.\frac{\partial A(\boldsymbol{z})}{\partial \boldsymbol{z}}\right|_{\boldsymbol{z}=\check{\boldsymbol{z}}} = -\left(\frac{\partial^2 J}{\partial \boldsymbol{x}^2}\right)^{-1}\left.\frac{\partial^2 J}{\partial \boldsymbol{z}\partial \boldsymbol{x}}\right|_{\boldsymbol{x}=A(\check{\boldsymbol{z}})} \quad (8)$$

By substituting this in (7) the thesis follows. ∎

Please note that the approximation depends only on the error function J being minimized by algorithm A; there are no hypotheses on A itself. The term $\partial^2 J/\partial \boldsymbol{x}\partial \boldsymbol{z}$ quantifies the variation of the error function caused by noise: this is the information that the methods described in Section II-B did not use.

IV. Application to ICP

It is very easy to apply the method. One must simply rewrite (2) as to show explicitly the contribution of each range measurement; then one computes the derivatives at the estimated $\hat{\boldsymbol{x}}$ and evaluates (6).

For each correspondence, there are three measurements that give a contribution. The reference surface S_{ref} is created by connecting the points in $\boldsymbol{y}_{t-1}$ with segments; each segment is created by two points. For the k-th correspondence, call i^k the index of the point in $\boldsymbol{y}_t$, and call j_1^k and j_2^k the indexes for the points in $\boldsymbol{y}_{t-1}$ that create the segment closest to $\mathbf{T}_{\boldsymbol{x}}\boldsymbol{p}_{i^k}^t$. By writing the points $\boldsymbol{p}$ in the polar form (for example: $\boldsymbol{p}_{i^k} = \tilde{\rho}_{i^k}\boldsymbol{v}_{i^k}$, where $\boldsymbol{v}_{i^k}$ is the direction of the sensor ray), one obtains J as a function of the readings:

$$J(\{\tilde{\rho}_j^{t-1}\},\{\tilde{\rho}_i^t\},\boldsymbol{x}) = \quad (9)$$
$$\sum_k \left\| \mathbf{T}_{\boldsymbol{x}}\tilde{\rho}_{i^k}^t\boldsymbol{v}_{i^k} - \Pi\Big(\mathrm{seg}(\tilde{\rho}_{j_1^k}^{t-1}\boldsymbol{v}_{j_1^k}, \tilde{\rho}_{j_2^k}^{t-1}\boldsymbol{v}_{j_2^k}), \mathbf{T}_{\boldsymbol{x}}\tilde{\rho}_{i^k}^t\boldsymbol{v}_{i^k}\Big)\right\|^2$$

The necessary derivatives ($\partial^2 J/\partial \boldsymbol{x}^2$ and $\partial^2 J/\partial \boldsymbol{x}\partial \boldsymbol{z}$) can easily be computed in closed form – they are not reported here for reasons of space. Evaluating (6) requires only some matrix multiplications (greatly simplified in the common case of a diagonal $\mathrm{cov}(\boldsymbol{z})$) and the inversion of a 3×3 matrix.

Please note that the method takes into account the fact that a measurement is involved in more than one correspondence, and that it does not assume that the measurements are uncorrelated: $\mathrm{cov}(\boldsymbol{z})$ can be a full matrix. Moreover it can handle the case of localization, by simply not considering S_{ref} as subject to uncertainty (using $\boldsymbol{z} = \boldsymbol{y}_t$ instead of $\boldsymbol{z} = \{\boldsymbol{y}_{t-1}, \boldsymbol{y}_t\}$).

A comment on the well-posedness of the problem. The implicit function theorem requires that $\partial^2 J/\partial \boldsymbol{x}^2$ be non singular. Assume that there are more than 3 correspondences: then in scan matching $\partial^2 J/\partial \boldsymbol{x}^2 > 0$ with probability 1,

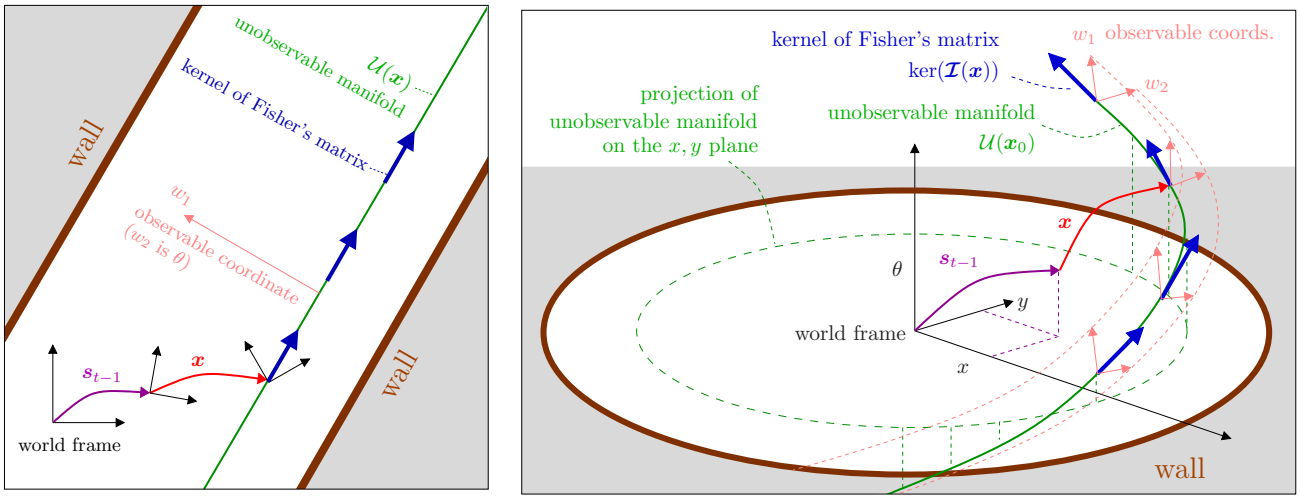

Fig. 3. In a bidimensional world, two kinds of under-constrained situations are possible [9]: the corridor environment and the circular environment. In the first case the unobservable manifold is a linear subspace, while in the second case it is a curve. In both case, the kernel of Fisher's information matrix is tangent to the unobservable manifold.

as the only situation in which it is singular is when all the segments in S_{ref} are parallel, and this is never true because measurements are noisy (in other words, $\{\boldsymbol{z} : \det(\partial^2 J/\partial \boldsymbol{x}^2) = 0\}$ is a set of measure 0 immersed in the space of measurements). Incidentally, this means that one can expect that (2) is a strictly convex problem even in under-constrained situations: in that case the ICP finds a minimum, but that is just fitting the noise. As for localization, $\det(\partial^2 J/\partial \boldsymbol{x}^2) = 0$ can indeed hold in some cases.

There are at least two ways to work around this problem. The first is to step back and recognize that localization and scan matching are *never* under-constrained, if an odometry estimate is present. Let $\boldsymbol{u}$ be the odometry estimate of $\boldsymbol{x}$ having a bounded covariance $\text{cov}(\boldsymbol{u})$. One can formulate a maximum-a-posteriori problem by adding a term to the error function, which weights the odometry information:

$$J_{\text{MAP}}(\boldsymbol{z}, \boldsymbol{u}, \boldsymbol{x}) = J(\boldsymbol{z}, \boldsymbol{x}) + (\boldsymbol{x} - \boldsymbol{u})^{\intercal} [\text{cov}(\boldsymbol{u})]^{-1} (\boldsymbol{x} - \boldsymbol{u}) \quad (10)$$

(this can be solved by ICP by introducing a dummy correspondence). Applying (6) to J_{MAP} and considering $\boldsymbol{u}$ as part of the measurements, one may conclude that the covariance of $\hat{\boldsymbol{x}}_{\text{MAP}}$ is bounded: $\text{cov}(\hat{\boldsymbol{x}}_{\text{MAP}}) \leq \text{cov}(\boldsymbol{u})$.

The second way, and the one that will be employed in the next section, is to explicitly detect the under-constrained direction by analyzing Fisher's information matrix, and then carry on the analysis on the observable manifold.

V. SIMULATIONS

The goal of the simulations was to compare the method with those proposed in [1]. Three cases are considered: the square, the corridor and a circular environment. The latter two exemplify the two kinds of under-constrained situations which may happen [9]; for those an observability analysis is performed. *Methodology:* The best way to think of the simulations is as Monte Carlo approximations to (1). Therefore, the values of $\boldsymbol{y}_t, \boldsymbol{y}_{t-1}, \boldsymbol{u}$ change, while the true $\boldsymbol{x}$ remains fixed. This is the simulation algorithm:

1) Choose the first pose $\boldsymbol{s}_{t-1}$. Choose a fixed true $\overline{\boldsymbol{x}}$. Let $\boldsymbol{s}_t = \boldsymbol{s}_{t-1} \oplus \overline{\boldsymbol{x}}$ be the second pose. These remain constant for all the simulations.
2) Repeat for $m = 1, 2, \ldots, 300$
   a) Create a noise-corrupted first scan $\boldsymbol{y}_{t-1}^m$ at $\boldsymbol{s}_{t-1}$.
   b) Create a noise-corrupted second scan $\boldsymbol{y}_t^m$ at $\boldsymbol{s}_t$.
   c) Sample a starting guess $\boldsymbol{u}^m \sim \mathcal{N}(\overline{\boldsymbol{x}}, \text{cov}(\boldsymbol{u}))$.
   d) Run ICP to obtain $\hat{\boldsymbol{x}}^m = A(\boldsymbol{y}_{t-1}^m, \boldsymbol{y}_t^m, \boldsymbol{u}^m)$
3) Compute $\text{cov}(\{\hat{\boldsymbol{x}}^m\})$ as an approximation to $\text{cov}(\hat{\boldsymbol{x}})$.

The experimental methodology is subtly different from that employed in [1]. Here the true $\boldsymbol{x}$ is fixed, while in [1] it changes. Another important difference is that in [1] the second scan is simulated on an approximated geometric map built on the first scan: this produces artificially good results for the Offline method.

For the rest, the parameters have been chosen as close as possible to those employed in [1], [2]. The sensor has 52 rays distributed on 360°; the noise is Gaussian with zero mean and a standard deviation of $0.03m$. The odometry error has covariance $\text{cov}(\boldsymbol{u}) = \text{diag}(0.35m, 0.35m, 7.5°)$.

a) The square environment (Fig. 4): The square is an example of a constrained environment. In Fig. 4 both the results for localization and for scan matching are shown.

As for localization, the Cramér–Rao bound and the proposed method provide a very close estimate to the true covariance. As for scan-matching, the pessimism of the Hessian method, as shown in [1], is confirmed. The Offline method has worse performance than in [1] as the methodology has been slightly changed. The proposed method provides an excellent approximation.

b) The corridor environment: This is the most common under-constrained situation encountered in practice: the robot cannot see the end of the corridor and on the sides there are

no useful features. To treat this situation, one must recognize that there is an unobservable direction, and then carry on the comparison of the methods on the observable manifold. Only the projection of the errors on the observable manifold are significant. The Appendix recalls the definition of $\boldsymbol{\mathcal{I}}(\boldsymbol{x})$, the Fisher's information matrix for localization. In an under-constrained situation, one eigenvalue of $\boldsymbol{\mathcal{I}}(\boldsymbol{x})$ is close to zero. The corresponding eigenvector $p_u(\boldsymbol{x})$ defines the unobservable subspace $\mathcal{U}(\boldsymbol{x}) = \text{span}\{p_u(\boldsymbol{x})\}$; while the other two define the observable subspace $\mathcal{O}(\boldsymbol{x}) = \text{span}\{p_1(\boldsymbol{x}), p_2(\boldsymbol{x})\}$.

To ignore the components of the errors which lie in $\mathcal{U}(\boldsymbol{x})$ and are not observable, one should project the errors from the (x, y, θ) space to $\mathcal{O}$. Define $\boldsymbol{T}(\boldsymbol{x})$ as a projector from $\mathbb{R}^2 \times [0, 2\pi)$ to $\mathcal{O}$: $\boldsymbol{T}(\boldsymbol{x}) \triangleq [p_1(\boldsymbol{x})\ p_2(\boldsymbol{x})]^{\mathrm{T}}$. The error samples are projected with $\boldsymbol{w} = \boldsymbol{T}(\overline{\boldsymbol{x}})(\boldsymbol{x} - \overline{\boldsymbol{x}})$, and the covariances estimated by the different approaches can be projected using: $\text{cov}(\boldsymbol{w}) = \boldsymbol{T}(\overline{\boldsymbol{x}})\text{cov}(\hat{\boldsymbol{x}})\boldsymbol{T}(\overline{\boldsymbol{x}})^{\mathrm{T}}$. Finally, one can compare the actual errors on $\mathcal{O}$ with the projection of the estimated covariances. The Hessian method and the proposed method match the actual covariance well; the Offline method is moderately optimistic.

c) The circular environment (Fig. 4): The difference with respect to the corridor is that now the projection of the samples on the observable manifold is a non-linear transform. The unobservable manifold $\mathcal{U}(\boldsymbol{x})$, containing all the points which are not distinguishable from $\boldsymbol{x}$, can be parameterized by a number ϕ: $\mathcal{U}(\boldsymbol{x}) \triangleq \{[\boldsymbol{R}(\phi)\boldsymbol{t},\ \theta + \phi] \text{ for } \phi \in [0, 2\pi)\}$. $\mathcal{U}(\boldsymbol{x})$ is a spiral in the (x, y, θ) space, as shown in Fig. 3. At each point the kernel of $\boldsymbol{\mathcal{I}}(\boldsymbol{x})$ is tangent to $\mathcal{U}(\boldsymbol{x})$.

Also in this case the Hessian and the proposed method give similar results: they are both moderately optimistic with respect to the true error. The Offline method is very pessimistic, probably because the the polyline map it uses is quite a bad approximation for a circular environment.

The results can be summarized as follows:

	Square	Corridor*	Circle*
Hessian [1]	pessimistic	good	moderately optimistic
Offline [1]	good	moderately optimistic	pessimistic
proposed	very good	good	moderately optimistic

*: projection on the observable manifold

VI. Conclusions

This paper presented a method for estimating the covariance of the ICP algorithm, based on the analysis of the error function being minimized. It has been shown that under-constrained cases can be detected by examining the Fisher's information matrix. In such cases the proposed method accounts for the errors on the observable manifold. In the simulations, the proposed algorithm performed better than existing approaches, and the computational load is negligible with respect to the ICP algorithm itself.

Acknowledgements: thanks to Javier Minguez for insightful comments on a draft of this paper.

Appendix

A. Implicit function theorem

Let S an open set of $\mathbb{R}^{n+h}$ and $F = F(\boldsymbol{x}, \boldsymbol{z})$ a function from S to $\mathbb{R}^h$ of class C^1. Let $(\boldsymbol{x}_0, \boldsymbol{z}_0)$ be a point in S such that $F(\boldsymbol{x}_0, \boldsymbol{z}_0) = 0$, and $\det(\partial F(\boldsymbol{x}_0, \boldsymbol{z}_0)/\partial \boldsymbol{x}) \neq 0$. Then there exists a neighborhood I of $\boldsymbol{z}_0$, a neighborhood J of $\boldsymbol{x}_0$ and a unique function $f : I \subset \mathbb{R}^n \to J \subset \mathbb{R}^h$ such that $\boldsymbol{x}_0 = f(\boldsymbol{z}_0)$ and $F(f(\boldsymbol{z}), \boldsymbol{z}) = 0 \quad \forall \boldsymbol{z} \in I$. Moreover $f \in C^1$ and $\partial f(\boldsymbol{z})/\partial \boldsymbol{z} = -\left[\partial F(\boldsymbol{z}, f(\boldsymbol{z}))/\partial \boldsymbol{x}\right]^{-1} \partial F(f(\boldsymbol{z}), \boldsymbol{z})/\partial \boldsymbol{z}$.

B. Fisher's information matrix for localization

In [9] it is derived the Fisher's information matrix for localization:

$$\boldsymbol{\mathcal{I}}(\boldsymbol{x}) = \frac{1}{\sigma^2} \sum_i \begin{bmatrix} \frac{\boldsymbol{v}(\alpha_i)\boldsymbol{v}(\alpha_i)^{\mathrm{T}}}{\cos^2 \beta_i} & r_i \frac{\tan \beta_i}{\cos \beta_i} \boldsymbol{v}(\alpha_i) \\ * & r_i^2 \tan^2 \beta_i \end{bmatrix} \tag{11}$$

where α_i is the direction of the normal to the surface at the sensed point, β_i is the incidence angle (angle between the normal to the surface and the sensor ray) and r_i is the expected sensor reading. The inverse of $\boldsymbol{\mathcal{I}}(\boldsymbol{x})$ is the Cramér–Rao bound for unbiased estimators for localization ($\text{cov}(\hat{\boldsymbol{x}}) \geq [\boldsymbol{\mathcal{I}}(\boldsymbol{x})]^{-1}$). In an under-constrained situation $\boldsymbol{\mathcal{I}}(\boldsymbol{x})$ is singular, and the kernel gives the direction of the uncertainty. As for $\boldsymbol{\mathcal{I}}_{\text{SM}}(\boldsymbol{x})$, the corresponding matrix for scan matching, it is difficult to obtain a closed form [9]. However, because scan matching is the very same problem as localization, but *with less information*, one may conclude that $\boldsymbol{\mathcal{I}}_{\text{SM}}(\boldsymbol{x}) \leq \boldsymbol{\mathcal{I}}(\boldsymbol{x})$. Because $\ker(\boldsymbol{\mathcal{I}}_{\text{SM}}(\boldsymbol{x})) \supset \ker(\boldsymbol{\mathcal{I}}(\boldsymbol{x}))$, it makes sense to consider the kernel of $\boldsymbol{\mathcal{I}}(\boldsymbol{x})$ as the under-constrained directions for scan matching as well.

References

[1] O. Bengtsson and A.-J. Baerveldt, "Robot localization based on scan-matching — estimating the covariance matrix for the IDC algorithm," *Robotics and Autonomous Systems*, vol. 44, pp. 29–40, July 2003.

[2] O. Bengtsson, *Robust Self-Localization of Mobile Robots in Dynamic Environments Using Scan Matching Algorithms*. PhD thesis, Department of Computer Science and Engineering, Chalmers University of Technology, Göteborg, Sweden, 2006. ISBN 91-7291-744-X.

[3] S. Rusinkiewicz and M. Levoy, "Efficient variants of the ICP algorithm," in *Int. Conf. on 3D Digital Imaging and Modeling (3DIM)*, 2001.

[4] F. Lu and E. Milios, "Robot pose estimation in unknown environments by matching 2D range scans," *Journal of Intelligent Robotics Systems*, vol. 18, no. 3, pp. 249–275, 1997.

[5] S. Pfister, K. Kriechbaum, S. Roumeliotis, and J. Burdick, "Weighted range sensor matching algorithms for mobile robot displacement estimation," in *Proc. of the IEEE Int. Conf. on Robotics and Automation (ICRA)*, 2002.

[6] J. Minguez, F. Lamiraux, and L. Montesano, "Metric-based scan matching algorithms for mobile robot displacement estimation," *IEEE Transactions on Robotics*, 2006.

[7] P. Biber and W. Strasser, "The normal distributions transform: A new approach to laser scan matching," in *Proc. of the IEEE/RSJ Int. Conf. on Intelligent Robots and Systems (IROS)*, 2003.

[8] J. Nieto, T. Bailey, and E. Nebot, "Scan-SLAM: Combining EKF-SLAM and scan correlation," in *Fifth Int. Conf. on Field Robotics (FSR)*, (Port Douglas, Australia), July 2005.

[9] A. Censi, "On achievable accuracy for range-finder localization," in *Proc. of the IEEE Int. Conf. on Robotics and Automation (ICRA)*, 2007.

[10] F. Lu, *Shape registration using optimization for mobile robot navigation*. PhD thesis, Department of C.S., University of Toronto, 1995.

[11] A. R. Chowdhury and R. Chellappa, "Stochastic approximation and rate distortion analysis for robust structure and motion estimation," *International Journal of Computer Vision*, pp. 27–53, October 2003.

SQUARE ENVIRONMENT

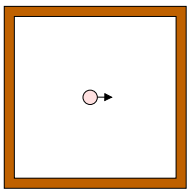

Localization errors (*mm,mm,°*)			
	$\sigma(x)$	$\sigma(y)$	$\sigma(\theta)$
true	5.3	5.3	0.039
CRB	5.1	5.3	0.037
proposed	5.4	5.4	0.042

Scan matching errors (*mm,mm,°*)			
	$\sigma(x)$	$\sigma(y)$	$\sigma(\theta)$
true	7.6	7.8	0.058
Hessian	20.0	20.3	0.171
Offline	7.0	6.8	0.086
proposed	7.7	7.7	0.060

ERRORS FOR LOCALIZATION (matching a noisy sensor scan against a perfect map)

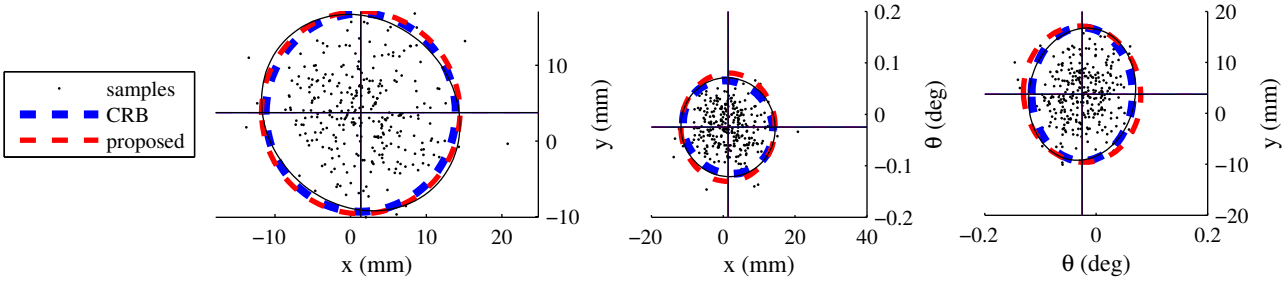

ERRORS FOR SCAN MATCHING (matching two noisy sensor scans)

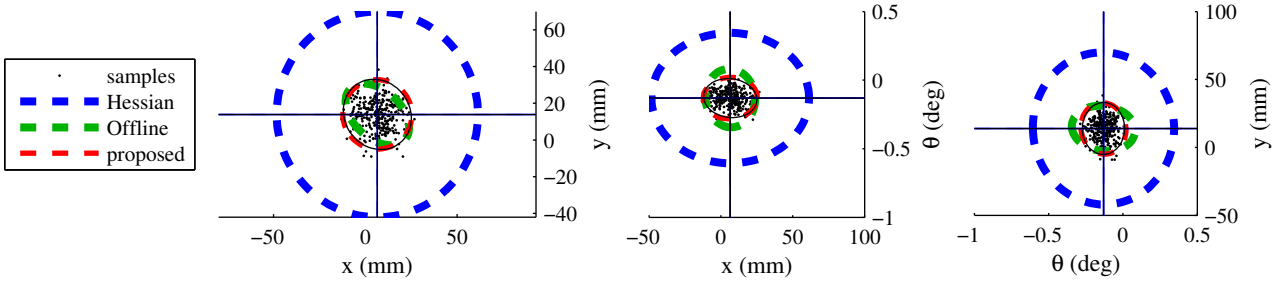

CORRIDOR ENVIRONMENT

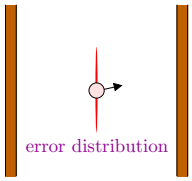

Scan matching errors (*mm,mm,°*)				Projected on $\mathcal{O}$ $\longrightarrow$	
	$\sigma(x)$	$\sigma(y)$	$\sigma(\theta)$	$\sigma(w_1)$	$\sigma(w_2)$
true	38	219	0.22	0.84	0.38
Hessian	33	186	0.24	0.94	0.42
Offline	50	273	0.14	0.63	0.26
proposed	40	257	0.19	0.84	0.33

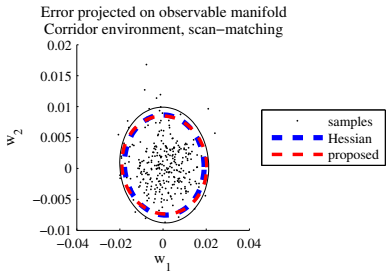

CIRCULAR ENVIRONMENT

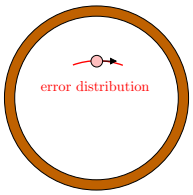

Scan matching errors (*mm,mm,°*)				Projected on $\mathcal{O}$ $\longrightarrow$	
	$\sigma(x)$	$\sigma(y)$	$\sigma(\theta)$	$\sigma(w_1)$	$\sigma(w_2)$
true	284	31	8.2	1.50	0.39
Hessian	13	7	0.3	0.78	0.36
Offline	378	43	5.6	3.27	8.37
proposed	13	9	0.3	0.84	0.36

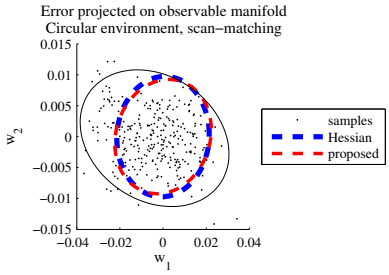

Fig. 4. The figure shows the results for localization and scan matching in three environments: the simple square and the two possible under-constrained environments: corridor and circle. **Square**: The three-dimensional data is shown projected on the three planes (x, y), (x, θ), (θ, y). In the picture the black dots are the actual error samples. The proposed method is very accurate, both for localization and scan matching, and much more accurate than the Hessian method (very pessimistic) and the Offline method. *Parameters*: The environment is a square with a $10m$ side. The first pose is at $\boldsymbol{s}_{t-1} = (0, 0, 0°)$ (center of the square), and the displacement is $\overline{\boldsymbol{x}} = (0.1m, 0, 2°)$. **Corridor:** In an under-constrained case, only the errors projected on the observable manifold are significant (right table and figure). The Hessian and the proposed method provide a good approximation of the covariance for the observable part of the state space. *Parameters*: The environment is a $10m$ square with two sides removed. $\boldsymbol{s}_{t-1} = (0, 0, 10°)$, $\overline{\boldsymbol{x}} = (0.1m, 0, 2°)$. **Circle:** In this case, the Offline method is pessimistic, and the Hessian and the proposed method are moderately optimistic. *Parameters*: The environment is a circle with a $5m$ radius. The first pose $\boldsymbol{s}_{t-1}$ is $(0, 2m, 0°)$, slightly off-centered; the displacement is $\overline{\boldsymbol{x}} = (0.1, 0, 2°)$.